Influence of wire mesh, and CFRP strengthening on blast performance of brick masonry wall: a numerical study under close-range explosion

Article *in* International Journal of Masonry Research and Innovation · October 2022

DOI: 10.1504/IJMRI.2022.10051479

CITATIONS
7

READS
104

5 authors, including:

Mohd Shariq
Jamia Millia Islamia
15 PUBLICATIONS **297** CITATIONS
SEE PROFILE

Mehtab Alam
Netaji Subhas University of Technology Delhi
129 PUBLICATIONS **2,260** CITATIONS
SEE PROFILE

S M Anas
Jamia Millia Islamia
58 PUBLICATIONS **1,445** CITATIONS
SEE PROFILE

Asif Husain
Jamia Millia Islamia
19 PUBLICATIONS **161** CITATIONS
SEE PROFILE

Influence of wire mesh, and CFRP strengthening on blast performance of brick masonry wall: a numerical study under close-range explosion

Mohd Shariq*

Department of Civil Engineering,
Faculty of Engineering and Technology,
Jamia Millia Islamia (A Central University),
New Delhi, 110 025, India
Email: shariqqq786@gmail.com
*Corresponding author

Mehtab Alam

Department of Civil Engineering,
Netaji Subhas University of Technology (West Campus),
New Delhi, 110 073, India
Email: mehtab.alam@nsut.ac.in

S.M. Anas, Asif Hussain and Nazrul Islam

Department of Civil Engineering,
Faculty of Engineering and Technology,
Jamia Millia Islamia (A Central University),
New Delhi, 110 025, India
Email: mohdanas43@gmail.com
Email: ahusain2@jmi.ac.in
Email: nazrulislam.jmi@gmail.com

Abstract: A common structural member in the buildings used for both commercial and residential formats is load-bearing brick masonry walls. In this study, a finite-element model of unreinforced brick-masonry wall, 1,600 mm × 2,100 mm × 240 mm, is developed, analysed, and validated with the available test results using the ABAQUS/Explicit-v.6.15 code under 5 kg-TNT load at scaled distance 0.58 m/kg$^{1/3}$. To improve the wall response, it has been strengthened with: 1) wire mesh of different thicknesses 2.50 mm, 3.50 mm, and 4.50 mm on the rear face only and on both the faces of the wall; 2) CFRP wrapping with 0.50 mm and 0.60 mm thick on the rear face only and 0.30 mm thick on both the faces of the wall. Equivalent thickness of the wrapping to the steel wire-mesh from displacement and damage point of view is evaluated. CFRP-strengthened walls displayed better performance than walls with wire-mesh with regards to damage and displacement.

Keywords: brick masonry; blast loading; CFRP; damage; load-bearing structures; micro-modelling; strain-rate effects; wire mesh.

Reference to this paper should be made as follows: Shariq, M., Alam, M., Anas, S.M., Hussain, A. and Islam, N. (xxxx) 'Influence of wire mesh, and CFRP strengthening on blast performance of brick masonry wall: a numerical study under close-range explosion', *Int. J. Masonry Research and Innovation*, Vol. X, No. Y, pp.xxx–xxx.

Biographical notes: Mohd Shariq currently works as a PhD scholar at the Department of Civil Engineering, Faculty of Engineering and Technology, Jamia Millia Islamia, New Delhi, India. His qualifications comprise of a Bachelors of Technology (Civil) and Masters of Technology (Earthquake Engineering) with honours. He is a Civil Engineer with great experience in structural analysis, blast simulation, and finite element modelling. Their current project is 'blast analysis of masonry compression members'.

Mehtab Alam is currently a Professor Emeritus in the Civil Engineering Department, Netaji Subhas University of Technology, West Campus, New Delhi-110073. He is a member of several societies such as the Indian Society of Earthquake Technology (IIT-Roorkee), the Indian Society of Technical Education, the Ferro cement Society of India, and so on. His teaching and research are in structural behaviour and design, structural mechanics, construction materials, recycling of demolished concrete waste, skin-reinforced concrete, earthquake disaster, and crisis-management with emphasis on RC slab systems, FRP concrete materials and their structural applications, structural safety and design code development.

S.M. Anas is a PhD scholar at the Department of Civil Engineering within the Faculty of Engineering and Technology, Jamia Millia Islamia (A Central University), Jamia Nagar, New Delhi, 110 025, India. He has a Bachelors of Technology (Civil) degree from the Sharda University and Masters of Technology (Earthquake Engineering) degree with honours from the Jamia Millia Islamia. His research interests are strengthening techniques, finite element modelling, structural performance, composite materials, FRP, AFRP, BFRP, C-FRP, GFRP, steel tubes, metallic foams, pre-tensioned concrete girders, blast-resistant shelters, heritage masonry buildings, masonry walls, underground blasting, ground shock, impact-resistant structures, impulsive-loadings, among others.

Asif Hussain is a Professor at the Department of Civil Engineering within the Faculty of Engineering and Technology, Jamia Millia Islamia (A Central University), Jamia Nagar, New Delhi, 110 025, India. His area of interest in research includes offshore structures, high rise buildings, structural dynamics, recycling of demolished concrete waste, seismic loading, concrete testing, and high-rise buildings.

Nazrul Islam is a Professor at the Department of Civil Engineering, Faculty of Engineering and Technology, Jamia Millia Islamia (A Central University), Jamia Nagar, New Delhi, 110 025, India. He received his BSc degree from the Aligarh Muslim University, UP, India in 1984. He received his MTech from IIT Roorkee and PhD in Structural Engineering from the Indian Institute of Technology, New Delhi, India in 1990 and 1998. His main research area includes dynamic response of offshore structures, vulnerability analysis of bridges and finite element modelling of structures.

1 Background

Explosions, whether accidental or planned, can cause significant damage to the built infrastructure and result in fatalities to occupants of buildings in close proximity to the centre of explosion. The increase in the number of terrorist attacks over the past few decades has led to growing concerns about the performance of buildings designed for aesthetics and economy when subjected to blast loading. The United States Federal Emergency Management Agency (FEMA) reports that approximately one in every two terrorist attacks involves the use of explosives (Ahmadi et al., 2021, 2022; Anas et al., 2020a, 2020b, 2020c, 2021a, 2021b, 2021c, 2021d, 2021f, 2021e, 2022a, 2022b, 2022c, 2022d, 2022e, 2022f, 2022g, 2022h, 2022i, 2022j, 2022k, 2022l, 2022m, 2022n, 2022o, 2022p; Anas and Alam, 2021a, 2021b, 2022a, 2022b, 2022c, 2022d, 2022e; Shariq et al., 2022a, 2022b, 2022c, 2022d, 2022e, 2022f; Tahzeeb et al., 2022a, 2022b, 2022c; Ul Ain et al., 2021, 2022; Aamir et al., 2022; Hao and Tarasov, 2008; Stewart and Lawrence, 2002). Thus, if a terrorist action is suspected, it is very likely to involve the use of explosives. Furthermore, the terrorist's attacks on the Alfred P. Murrah Building in Oklahoma City and the World Trade Centre in New York City and many more around the world have revealed the blast load vulnerability of buildings designed and constructed without due consideration to blast loading. Many researchers are, thus, seeking to understand the behaviour of structural elements under blast loading and to develop mitigation/retrofit measures to protect critical buildings and infrastructure systems against blast loading. Retrofitting an existing building for improved blast resistance can be expensive (Anas and Alam, 2022c, 2022d, 2022e, Anas et al., 2022c, 2022d, 2022e, 2022f, 2022g, 2022h, 2022i, 2022j, 2022m, 2022o, 2022p; Ahmadi et al., 2022; Shariq et al., 2022a, 2022c, 2022d, 2022f; Tahzeeb et al., 2022a, 2022b, 2022c; Ul Ain et al., 2021, 2022). However, as structures designed to resist one load type can often have capacity to resist a different load type, it is important to establish the blast resistance of structural elements designed for other load types, e.g., seismic loads. Buildings designed to meet strength and ductility requirements, depending on the seismicity of a particular region and the importance of the building, could have inherent capacity to resist blast loading (Ahmadi et al., 2021; Anas et al., 2020a, 2020b, 2020c, 2021a, 2021b, 2021c, 2021d, 2021e, 2021f, 2022a, 2022b, 2022k, 2022l, 2022n; Anas and Alam, 2021a, 2021b, 2022a, 2022b; Aamir et al., 2022; Hao and Tarasov, 2008; Stewart and Lawrence, 2002; Shariq et al., 2022b, 2022e).

Unreinforced masonry constructions have negative consequences from impulsive loadings, which reduce their ability to handle axial loads. Masonry building is a traditional method that has been utilised to build infrastructure for economically disadvantaged groups in rural areas for a very long time (Anas et al., 2020a, 2020b, 2020c, 2021a, 2021b, 2021c, 2021d, 2021e, 2021f, 2022c, 2022d, 2022e, 2022f, 2022g, 2022h, 2022i, 2022j, 2022k, 2022m, 2022o, 2022p; Pandey and Bisht, 2014; Ahmadi et al., 2021, 2022; Anas and Alam, 2021a, 2021b, 2022c, 2022d, 2022e; Shariq et al., 2022a, 2022c, 2022d, 2022f; Tahzeeb et al., 2022a, 2022b, 2022c; Ul Ain et al., 2021, 2022; Milani and Lourenco, 2009; Milani et al., 2009; Aamir et al., 2022). Unreinforced masonry has a weak resistance to out-of-plane stress due to its brittle nature (Ehsani and Pena, 2009). At least one of the three prevalent forms of failures, namely tensile failure, compression failure in zones of severe flexure, and shear failure close to the support, are often present in masonry walls exposed to explosions (Myers et al., 2004). For academics

and engineers, the safety issue with masonry walls subjected to blast loading is a problem and a research area. The first technique is the traditional retrofitting procedure, in which steel and concrete are added to these walls to boost their strength (Anas et al., 2021d, 2021e; Badshah et al., 2021). The disadvantage of this approach is that it requires more time and money. However, employing C-FRP and other materials that are openly available in the literature, researchers have created and recognised new strengthening methods to improve the blast enhancement of masonry buildings (Shamim et al., 2019; Anas and Alam, 2022a, 2022b, 2022c, 2022d, 2022e, Anas et al., 2022a, 2022b, 2022c, 2022d, 2022e, 2022f, 2022g, 2022h, 2022i, 2022j, 2022l, 2022m, 2022n, 2022o, 2022p; Ahmadi et al., 2022; Shariq et al., 2022a, 2022b, 2022c, 2022d, 2022e, 2022f, 2022k; Tahzeeb et al., 2022a, 2022b, 2022c; Ul Ain et al., 2021, 2022; Milani and Lourenco, 2009; Milani et al., 2009; Aamir et al., 2022; Hao and Tarasov, 2008; Stewart and Lawrence, 2002).

2 Literature survey

Hao and Tarasov (2008) conducted dynamic uniaxial compressive tests to study the strain rate effect of brick and mortar materials. They found that the compressive strength of brick and mortar increases significantly with the strain rate. Stewart and Lawrence (2002) developed a method to calculate the structural reliability of typical masonry walls subject to vertical bending. They found that structural reliabilities are very sensitive to wall width, workmanship, and discreteness of masonry unit thickness. As reported by Hao and Tarasov (2008); a reliable prediction of UBM structure response to blast loads requires an accurate material model. Such model should reflect the characteristics of brick and mortar behaviour at high strain rates.

A 100 kg TNT surface burst was studied by Pandey and Bisht (2014) at stand-off distances of 20 m, 30 m, and 40 m. Three grades of concrete mortar – 1:6, 1:4.5, and 1:3 – were investigated in the study on walls that were 340 and 235 millimetres thick and were infilled in RC frames. The RC frame's cross-section was 350 mm × 345 mm while the walls' length and height were also 3,000 mm. A further 13.46 MPa was the total strength of the brick, while 6.78 MPa, 13.86 MPa, and 24.80 MPa, respectively, were the strengths of the three grade mortars (1:6, 1:4.5, and 1:3). The RC frame's steel and concrete grades were M15 and Fe415, respectively. The study's findings showed that a 340 mm thick masonry wall had become unusable after blasting for three different classes of masonry at a blast force of 100 kg TNT at a 20 m detonation distance. Additionally, for all mortar grades that indicated re-usable masonry, the deflection was relatively lower for the case of a 40 m detonation distance. Two un-retrofitted masonry (URM) walls measuring 11 feet tall, 8 feet long, and 8 inches thick were created by Ehsani and Pena (2009) using conventional mortar mixture and 16 × 8 × 8-inch masonry blocks. The masonry's compressive strength was 1,500 psi (10.34 MPa). C-FRP was adapted onto one URM wall on both sides. With a 30-foot standoff, a 200 pound (90.8 kilogrammes) TNT charge was detonated in front of the walls. According to the study's findings, an efficient application of C-FRP retrofitting prevented the collapse of the URM wall and kept all of the masonry rubble inside the C-FRP. Wu et al.'s (2021) experimental investigation used eight clay brick masonry walls that were each 2.1 × 1.6 × 0.24 metres in size. The bricks used in the masonry walls have dimensions of 240 mm × 115 mm × 53 mm and a compressive strength of 15.5 MPa. The mortar used in the construction had a

10 mm thickness and was estimated to have an average compressive strength of 4.9 MPa. On both sides of the wall, 10 mm of plaster was first laid, then a 3 mm layer of polyurea. A 5 kg TNT blast load was applied to the wall at three different standoff distances: 1.5 m, 1 m, and 0.6 m. The study found that applying a polyurea coating considerably increased the walls' ability to withstand blasts, with the effect being greater on the back face of the walls than the front (Hadi Ghaffoori Kanaan et al., 2022; Kanaan and Abdullah, 2021; Kanaan and Khashan, 2022; Kanaan, 2018, 2021; Kanaan et al., 2020a, 2020b, 2021; Kanaan and Tarek, 2020; Kanaan and Abdulwahid, 2019; Kanaan and Al-Isawi, 2019).

A brick-wall with dimensions of 2,656 mm in height and 3,590 mm in length was given a numerical analysis by Wei and Stewart (2010), and its thickness was divided into three separate ranges: 110 mm, 230 mm, and 350 mm. The bricks used to construct the wall were 230 mm by 110 mm by 76 mm in size. Additionally, three different grades of mortars (B40, B30, and B20) and three different grades of bricks (B40, B30, and B20) were utilised (M5, M10, and M15). 10 mm was the mortar's thickness. A 125 kg TNT explosion charge was employed at varied stand-off distances of 20 metres, 25 metres, and 30 metres to measure the blast reaction of the wall. The investigation came to the conclusion that the structural response to large-scale blast loads was unaffected by the mortar strength and brick strength. Wei et al.'s (2021) investigation of a brick masonry wall of 1,250 mm by 1,490 mm by 240 mm employed bricks with dimensions of 240 mm by 115 mm by 53 mm. The mortar was 10 mm thick, and the brick had a compressive strength of 2.6 MPa. The mortar material's primary tensile stress at failure was estimated to be 1 MPa. The explosive charge used in the study was a C4 spherical charge, which had radii of 42.10 mm, 53.04 mm, 66.82 mm, and 84.19 mm and was evaluated at varied magnitudes of 0.5 kg, 1 kg, 2 kg, and 4 kg. To cause these explosives to detonate, they were placed in the centre of the brick masonry wall's front surface. The experiment came to the conclusion that a circular crater is created when a contact explosion caused by a spherical explosive charge emerges on a brick masonry wall, and its cross-sectional dimensions repeatedly grow as the radius increases. Myers et al. (2004) evaluated the blast response of two different types of brick walls, measuring 2.24 m in height and 1.22 m in length, with thicknesses of 102 mm and 203 mm. Two core hollow concrete blocks with nominal dimensions of 102 mm × 203 mm × 305 mm and 203 mm × 203 mm × 406 mm were used to build the walls. These two hollow concrete blocks have compressive strengths of 10.34 MPa and 12.48 MPa, respectively. Mortar had an average compressive strength of 10.34 MPa. Three alternative methods of wall reinforcement were used during the trial. In the first method, 6.4 mm GFRP rods were used at each horizontal junction to reinforce the wall. In the second, three 64 mm wide GFRP strips were used to support the wall vertically. In the final method, GFRP rods and GFRP strips were both used to reinforce the wall. 2.3 kg of PETN blast charge was administered at various stand-off distances ranging from 0.91 m to 3.66 m in order to study the explosion reaction. According to the study's findings, FRP composites gave significant advantages in strengthening masonry walls to withstand blast loads.

Unreinforced, ferro-cement overlay, and restricted masonry, all measuring 23 mm thick, was the subject of an experimental investigation started by Badshah et al. (2021). The wall was 1.83 metres high at this location. Bricks used in construction had dimensions of 23 × 11.40 × 7.60 cm, and masonry had a 3.13 MPa compressive strength. The ferro-cement overlay masonry wall received a coating of ferro-cement that was 19 mm thick. A constrained masonry wall was also reinforced longitudinally with four

bars of 12 mm each, and transversely with 8 mm stirrups spaced at 150 mm intervals. In the investigation, an expanding range of TNT equivalent charges were employed for the explosion, weighing anywhere between 0.56 kg and 17.8 kg, with a constant stand-off distance of 3.58 m. The experiment demonstrated that the danger of possible human fatalities and material losses was higher in the upper layers of a free-standing masonry wall constructed of ferro-cement overlay masonry and unreinforced bricks. Therefore, in unreinforced boundary masonry walls, precise strengthening procedures such as pre-compression should be applied to the top layers of the brick. A 3,000 mm × 230 mm masonry infilled wall was the subject of an investigation by Shamim et al. (2019). The RCC frame's cross-section, which was taken into account for modelling, was 230 mm × 235 mm. In addition, the wall contained a 1,000 × 1,000 mm hole. A 100 kg TNT charge was used to blast the wall from different standoff distances of 20 metres, 30 metres, and 40 metres. The results of the experiment showed that the peak displacement in the masonry walls with and without opening rose with decreasing stand-off distances, indicating that the blast's influence decreased with growing stand-off distances (Hadi Ghaffoori Kanaan et al., 2022; Kanaan and Abdullah, 2021; Kanaan and Khashan, 2022; Kanaan, 2018, 2021; Kanaan et al., 2020a, 2020b, 2021; Kanaan and Tarek, 2020; Kanaan and Abdulwahid, 2019; Kanaan and Al-Isawi, 2019).

3 Objectives of the current study

The goals of this research are:

- To analyse how the unreinforced masonry-wall responds dynamically to blast loads.
- To look at how C-FRP sheet and steel wire mesh affect how the wall responds to blasts.

4 Methodology for numerical modelling of brick masonry wall

In order to analyse the blast reaction of the clay brick masonry wall, which has dimensions of 2,100 mm (height) × 1,600 mm (length) × 240 mm, ABAQUS/CAE 2019 is being used (thickness). The brick's dimensions are as follows: 240 mm (length), 115 mm (width), and 53 mm (thickness) (Wu et al., 2021). The brick has the following parameters: 15.5 MPa in compressive strength, 1,800 kg/m^3 in density, 8,200 MPa in young modulus, 0.775 MPa in tensile strength, and 0.16 in poison ratio. These brick values were obtained from a research by Wu et al. (2021). On both faces of the brick masonry wall, a 10 mm thick coating of mortar is present. Other mortar characteristics have been extracted from Wu et al. (2021). Ten finite element models in all have been created for this investigation. The first finite element model (US) represents a conventionally un-strengthened wall, and the second, third, and fourth models are S-2.5-SWM-R, S-3.5-SWM-R, and S-4.5-SWM-R, respectively, where the first English letter 'S' stands for a strengthened wall, the second number indicates the diameter of the welded steel wire mesh (SWM), and the final letter 'R' indicates that the mesh is only applied to the wall' By adding more wire mesh to the front face of the first three models, the fifth, sixth, and seventh models – abbreviated S-2.5-SWM-B, S-3.5-SWM-B, and S-4.5-SWM-B – were created. The final 'B' stands for both faces. S-0.5-C-FRP-R and

S-0.6-C-FRP-R, the eighth and ninth versions, use 0.50 mm and 0.60 mm C-FRP sheets laminated to the wall's back face to reinforce the wall. Last but not least, the strengthening of the wall's front and rear faces, (i.e., S-0.3-C-FRP-B) has been accomplished utilising a 0.30 mm thick sheet of C-FRP. From Phan-Vu et al. (2021), the characteristics of C-FRP were extracted. For the welded steel wire mesh employed in the investigation, the mass density, yield strength, Young modulus, and Poisson's ratio were calculated as follows: 7,850 kg/m^3, 250 MPa, 210 GPa, and 0.3. In line with IS 4948 (2002), the welded steel wire mesh used in the aforementioned models has a 75 mm centre-to-centre spacing. 5 kilogramme of TNT was employed as the explosion charge weight in the investigation, and the stand-off distance was scaled to be 1.0 m (0.584 m/kg$^{1/3}$). The plaster is embedded with wire mesh using the embedded region constraint. To attach the wire mesh to the wall surface, use the tie constraint command. Wu et al.'s (2021) experimental test software includes a wall model that takes into account the boundary conditions and other factors.

4.1 Explosion loading

An explosion is defined as a large-scale, rapid and sudden release of energy. Explosions can be categorised on the basis of their nature as physical, nuclear or chemical events (Ahmadi et al., 2021, 2022; Anas et al., 2020a, 2020b, 2020c, 2021a, 2021b, 2021c, 2021d, 2021f, 2021e, 2022a, 2022b, 2022c, 2022d, 2022e, 2022f, 2022g, 2022h, 2022i, 2022j, 2022k, 2022l, 2022m, 2022n, 2022o, 2022p; Anas and Alam, 2021a, 2021b, 2022a, 2022b, 2022c, 2022d, 2022e; Shariq et al., 2022a, 2022b, 2022c, 2022d, 2022e, 2022f; Tahzeeb et al., 2022a, 2022b, 2022c; Ul Ain et al., 2021, 2022; Aamir et al., 2022; Hao and Tarasov, 2008; Stewart and Lawrence, 2002). In physical explosions, energy may be released from the catastrophic failure of a cylinder of compressed gas, volcanic eruptions or even mixing of two liquids at different temperatures. In a nuclear explosion, energy is released from the formation of different atomic nuclei by the redistribution of the protons and neutrons within the interacting nuclei, whereas the rapid oxidation of fuel elements (carbon and hydrogen atoms) is the main source of energy in the case of chemical explosions. Explosive materials can be classified according to their physical state as solids, liquids or gases. Solid explosives are mainly high explosives for which blast effects are best known (Anas and Alam, 2022a, 2022b, 2022c, 2022d, 2022e, Anas et al., 2022a, 2022b, 2022c, 2022d, 2022e, 2022f, 2022g, 2022h, 2022i, 2022j, 2022k, 2022l, 2022m, 2022n, 2022o, 2022p; Ahmadi et al., 2022; Shariq et al., 2022a, 2022c, 2022d, 2022f; Tahzeeb et al., 2022a, 2022b, 2022c; Ul Ain et al., 2021, 2022; Aamir et al., 2022; Hao and Tarasov, 2008; Stewart and Lawrence, 2002; Shariq et al., 2022b, 2022e). They can also be classified on the basis of their sensitivity to ignition as secondary or primary explosive. The latter is one that can be easily detonated by simple ignition from a spark, flame or impact. Materials such as mercury fulminate and lead azide are primary explosives. Secondary explosives when detonated create blast (shock) waves which can result in widespread damage to the surroundings. Examples include trinitrotoluene (TNT) and ANFO. The detonation of a condensed high explosive generates hot gases under pressure up to 300 kilo bar and a temperature of about 3,000°C–4,000°C. The hot gas expands forcing out the volume it occupies. As a consequence, a layer of compressed air (blast wave) forms in front of this gas volume containing most of the energy released by the explosion. Blast wave instantaneously

increases to a value of pressure above the ambient atmospheric pressure. This is referred to as the side-on overpressure that decays as the shock wave expands outward from the explosion source (Ahmadi et al., 2021, 2022; Anas et al., 2020a, 2020b, 2020c, 2021a, 2021b, 2021c, 2021d, 2021f, 2021e, 2022a, 2022b, 2022c, 2022d, 2022e, 2022f, 2022g, 2022h, 2022i, 2022j, 2022k, 2022l, 2022m, 2022n, 2022o, 2022p; Anas and Alam, 2021a, 2021b, 2022a, 2022b, 2022c, 2022d, 2022e; Shariq et al., 2022a, 2022b, 2022c, 2022d, 2022e, 2022f; Tahzeeb et al., 2022a, 2022b, 2022c; Ul Ain et al., 2021, 2022; Aamir et al., 2022; Hao and Tarasov, 2008; Stewart and Lawrence, 2002). After a short time, the pressure behind the front may drop below the ambient pressure. During such a negative phase, a partial vacuum is created and air is sucked in. This is also accompanied by high suction winds that carry the debris for long distances away from the explosion source.

The explosion is a catastrophic wave of highly compressed air or energy that spreads outward, causing a violent crushing of volume. The emission of hot, heavy, high-pressure gases at high temperatures often initiates this process (Ahmadi et al., 2021, 2022; Anas et al., 2020a, 2020b, 2020c, 2021a, 2021b, 2021c, 2021d, 2021f, 2021e, 2022c, 2022d, 2022e, 2022f, 2022g, 2022h, 2022i, 2022j, 2022m, 2022o, 2022p; Anas and Alam, 2021a, 2021b, 2022c, 2022d, 2022e; Shariq et al., 2022a, 2022c, 2022d, 2022f; Tahzeeb et al., 2022a, 2022b, 2022c; Ul Ain et al., 2021, 2022). A strong oxidation process that results in an explosion triggered by a blast releases a significant amount of energy in the form of light, heat, and sound for a brief yet devastating period of time. The blast pressure profile is illustrated in Figure 1 and starts with a value of atmospheric pressure (Anas and Alam, 2021a; Anas et al., 2021a, 2022c, 2022d, 2022e, 2022f, 2022g, 2022h, 2022i, 2022j, 2022m, 2022o, 2022p; Goel and Matsagar, 2014; Hao et al., 2016; Wu and Hao, 2005; Anas and Alam, 2022c, 2022d, 2022e; Ahmadi et al., 2022; Shariq et al., 2022a, 2022c, 2022d, 2022f; Tahzeeb et al., 2022a, 2022b, 2022c; Ul Ain et al., 2021, 2022). The symbol t_A indicates how long it took the blast wave to get to the area of interest (Time of arrival). The explosion takes place at time t_A, leading to an instantaneous rise in pressure, which is shown by P_i (peak over-pressure), for a very brief period of time. The P_i (peak over-pressure) is extremely important to employ on the blast face since it has the biggest magnitude during the entire blast event. The term t_d in the equation stands for the amount of time that the pressure has been greater than the atmospheric pressure (Anas et al., 2020b, 2020c, 2021c; Hao et al., 2016). After a brief period of time, the pressure of time begins to fall down exponentially, bringing the values of pressure and atmospheric pressure to a point where they are equal. As the value of pressure steadily decreases and eventually equals the value of atmospheric pressure, the vacuum is created and the pressure goes negative (Ahmadi et al., 2021; Anas et al., 2021b; Goel and Matsagar, 2014; Wu and Hao, 2005). Negative phase duration is the amount of time that the pressure has been lower than the atmospheric pressure. The theory of the time history of air blast wave pressure of the blast mechanism was clarified by Wu and Hao (2005), who also offered an empirical method to determine the values of air blast wave variables such as arrival time, rising time, and positive phase length.

$$t_A = 0.34 S^{1.4} W^{-0.2} / C_a \tag{1}$$

Here, W = Explosive charge (kg); S = detonation distance (m); C_a = speed of sound in air = 340 m/sec; t_A = arrival time of blast wave (sec).

$$t_1 = 0.0019\left(\frac{s}{w^{0.33}}\right)^{1.30} \tag{2}$$

$$t_2 = 0.0005S^{0.72}W^{0.16} \tag{3}$$

$$t_d = t_1 + t_2 \tag{4}$$

$$P(t) = \begin{Bmatrix} P_a, & (0 \le t \le t_A) \\ P_a + P_i\left(\frac{t}{t_i}\right), & (t_A \le t \le t_1) \\ P_a + P_i\left(1 - \frac{t-t_1}{t_2}\right).\exp\left(-\frac{\xi(t-t_1)}{t_2}\right), & (t_1 \le t) \end{Bmatrix} \tag{5}$$

Here, t_1 = rising time (sec); t_d = duration of positive phase (sec); t_2 = decreasing time (sec); P_a = atmospheric pressure 0.1 MPa; P_i = peak overpressure (MPa); ξ = decay coefficient.

$$\xi = \begin{Bmatrix} 3.02P_i^{0.38} + 6.85P_i^{0.79}.\exp\left(-4.55\frac{t-t_1}{t_2}\right), & (t_1 \le t \le t_d) \\ 1.96P_i^{0.25} + 0.176P_i.\exp\left(-0.73P_i^{-0.49}.\left(\frac{t-t_d}{t_2}\right)\right), & (t_d < t) \end{Bmatrix} \tag{6}$$

For $P_i \le 1.0$ and

$$\xi = \begin{Bmatrix} 1.62P_i^{0.30} + 5.13P_i^{0.28}.\exp\left(-1.05P^{0.37}.\left(\frac{t-t_1}{t_2}\right)\right), & (t_1 \le t \le t_d) \\ 0.74P_i^{0.17} + 2.71P_i^{0.28}.\exp\left(-0.26P_i^{0.33}.\left(\frac{t-t_1}{t_2}\right)\right), & (t_d < t) \end{Bmatrix} \tag{7}$$

For $1 < P_i \le 100$.

TM 5-1300 (1990), ASCE/SEI 59-11 (2011), and other blast design standards say that only positive pressure phase can be used for the assessment and planning of the concrete structure. The guidelines were created with the observation and findings of various studies and investigations in mind. These studies and investigations revealed that the value of the negative (suction) pressure phase is considerably less than atmospheric pressure, so it has no significant impact on the design of the structure (Ahmadi et al., 2021, 2022; Anas et al., 2020a, 2020b, 2020c, 2021a, 2021b, 2021c, 2021d, 2021f, 2021e, 2022c, 2022d, 2022e, 2022f, 2022g, 2022h, 2022i, 2022j, 2022k, 2022m, 2022o, 2022p; Anas and Alam, 2021a, 2021b, 2022c, 2022d, 2022e; Shariq et al., 2022a, 2022b, 2022c, 2022d, 2022f; Tahzeeb et al., 2022a, 2022b, 2022c; Ul Ain et al., 2021, 2022; Aamir et al., 2022). It has also been thought that these values disregard the damage reactions. As a result, it is recommended to disregard the negative pressure phase when designing structures and only consider the positive phase, as shown in Figure 1.

Figure 1 (a) Idealised history of blast (Wu and Hao, 2005) (b) Measured profile for 5 kg-TNT (Wu et al., 2021) (see online version for colours)

Comment [t1]: Author: Please provide a clearer version of this figure (preferably EPS file).

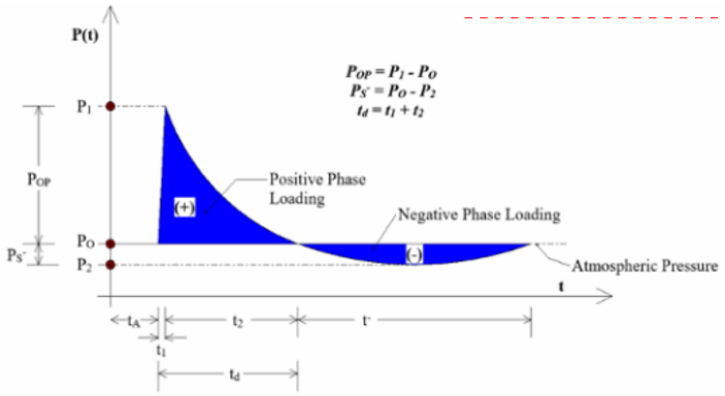

(a)

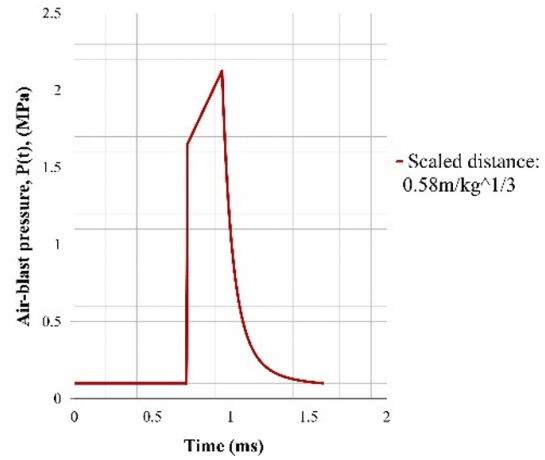

(b)

4.2 Damage model

A concrete damage model based on plasticity is known as the concrete damage plasticity (CDP) model. The model is used to design concrete and quasi-brittle materials that are taken into account in many sorts of structures, such as beams, columns, trusses, plates, and solids (Ahmadi et al., 2021, 2022; Anas et al., 2020a, 2020b, 2020c, 2021a, 2021b, 2021c, 2021d, 2021f, 2021e, 2022c, 2022d, 2022e, 2022f, 2022g, 2022h, 2022i, 2022j, 2022k, 2022m, 2022o, 2022p; Anas and Alam, 2021a, 2021b, 2022c, 2022d, 2022e; Shariq et al., 2022a, 2022b, 2022c, 2022d, 2022f; Tahzeeb et al., 2022a, 2022b, 2022c; Ul Ain et al., 2021, 2022; Aamir et al., 2022). The model uses the isotropic damage elasticity concept (ABAQUS/CAE FEA Program, 2017; Hafezolghorani et al., 2017; Voyiadjis et al., 2008) and displays inelastic behaviour of concrete. The CDP model

shows two different forms of concrete failures: compression crushing and tension cracking. The plasticity model may be used to depict these damages/cracks that are caused by the fracturing process in the model.

Figure 2 Concrete reaction (ABAQUS/CAE FEA Program, 2017) under a uniaxial loading condition: (a) compression (b) tension

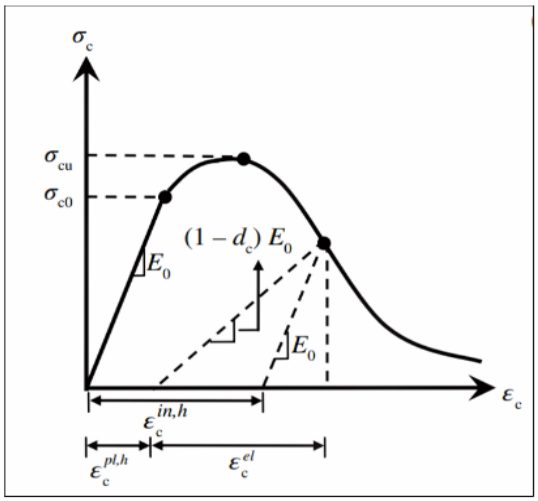

(a)

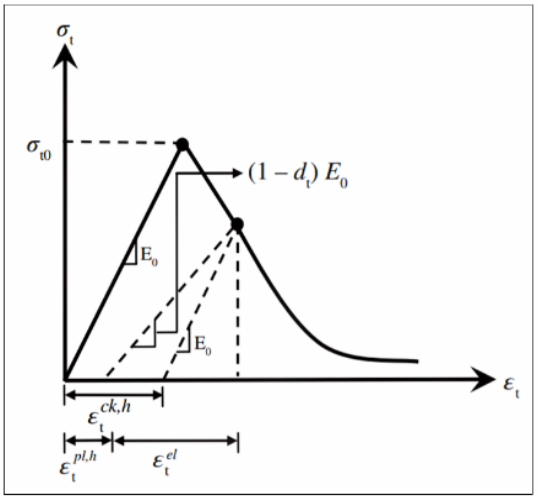

(b)

As seen in Figure 2, the damage plasticity is thought to be responsible for the concrete's uniaxial tensile and compressive response (ABAQUS/CAE FEA Program, 2017; Anas et al., 2020a; Voyiadjis et al., 2008). Up until the value of the failure stress reaches (σ_{t0}), the stress-strain response under uniaxial tension displays a linear relationship. When this

failure stress is exceeded, microcracks are created, which may be seen under a microscope using a stress-strain response (ABAQUS/CAE FEA Program, 2017; Anas and Alam, 2021b; Hafezolghorani et al., 2017). This strengthens the concrete structure's localisation of strain. The reaction in uniaxial compression stays linear until the initial yield value reaches (σ_{C0}) (ABAQUS/CAE FEA Program, 2017; Voyiadjis et al., 2008). Stress handling in the plastic area, followed by strain softening above the ultimate stress (σ_{cu}), serves as the primary indicators of response. Two hardening variables, $\epsilon_c^{pl,h}$ and $\epsilon_t^{pl,h}$, govern these failure surfaces. Uniaxial stress-strain curves are transformed into stress versus inelastic strain curves by ABAQUS/automated CAE's function (ABAQUS/CAE FEA Program, 2017; Hafezolghorani et al., 2017; Voyiadjis et al., 2008). Using statistical equations under compression and tensile loading in the CDP model, the uniaxial compression and tensile reactions of concrete are demonstrated. The following are the statistical formulae employed in the model:

$$\sigma_c = (1 - d_c) E_0 \left(\epsilon_c - \epsilon_c^{pl,h}\right) \tag{8}$$

Here, σ_c = nominal compressive stress (MPa), σ_{cu} = ultimate compressive stress (MPa), ϵ_c = compressive strain $(\epsilon_c^{pl,h} + \epsilon_c^{el})$, $\epsilon_c^{pl,h}$ = compressive equivalent plastic strain, ϵ_c^{el} = elastic compressive strain.

$$\sigma_t = (1 - d_t) E_0 \left(\epsilon_t - \epsilon_t^{pl,h}\right) \tag{9}$$

Here, σ_t = nominal tensile stress (MPa), σ_{t0} = failure stress (MPa), ϵ_t = tensile strain $(\epsilon_t^{pl,h} + \epsilon_t^{el})$, ϵ_t^{el} = elastic tensile strain. The model presupposes that a scalar degradation variable 'd', may be used to indicate how the material's modulus of elasticity has decreased.

$$E_a = (1 - d_{i=c,t}) E_0 \tag{10}$$

E_u = reduced modulus of elasticity (MPa), E_o = initial elasticity modulus of concrete (MPa), Damage parameters d_c and d_t range from zero to one (fully damaged material).

5 Results and discussion

The 240 mm thick brick masonry wall's fracture pattern under the assumed TNT load is determined to be in excellent agreement with the experimental findings, as shown in Figure 3. The wall's maximum transverse displacement is 275.24 mm, Figure 4, Figure 5, and Figure 6 show that the related damage dissipation energy, compressive, tensile, and shear stresses are 34,400 J, 121.42 MPa, 0.02 MPa, and 60.94 MPa. It is inferred that some of the bricks fall off the wall as observed in the trials from the estimated large transverse displacement (> wall thickness = 240 mm).

5.1 Response of wall strengthened with steel wire mesh on rear face only

- According to calculations, the walls' maximum transverse displacements, designated as S-2.5-SWM-R, S-3.5-SWM-R, and S-4.5-SWM-R, respectively, is 193.83 mm, 168.84 mm, and 156.65 mm, and their corresponding damage dissipation energies, indicated in Figure 4, are 19,160 J, 18,500 J, and 17,376 J.
- In comparison to the un-strengthened wall (US), Figure 6 shows that the compressive and shear stresses of the walls S-2.5-SWM-R, S-3.5-SWM-R, and S-4.5-SWM-R are reduced by 83.48%, 86.83%, and 86.04%, respectively, and by 83.30%, 89.46%, and 91.79%, respectively. The brittle reaction of the wall is caused by higher tension reinforcing.
- When steel wire mesh with diameters of 2.5 mm, 3.5 mm, and 4.5 mm is applied to a wall, the upper half of the mesh experiences tensile stresses of 250 MPa. However, according to Figure 7, the bottom half of the wire mesh's tensile stresses are 83.33 MPa and 41.67 MPa for horizontal wires with a diameter of 2.5 mm and 3.5 mm/4.5 mm, respectively.
- The wall is strengthened with steel wire mesh reinforcement, which increases the wall's stiffness and integrity against blast loading (Figure 5).

Figure 3 Wall-US crack pattern comparison (see online version for colours)

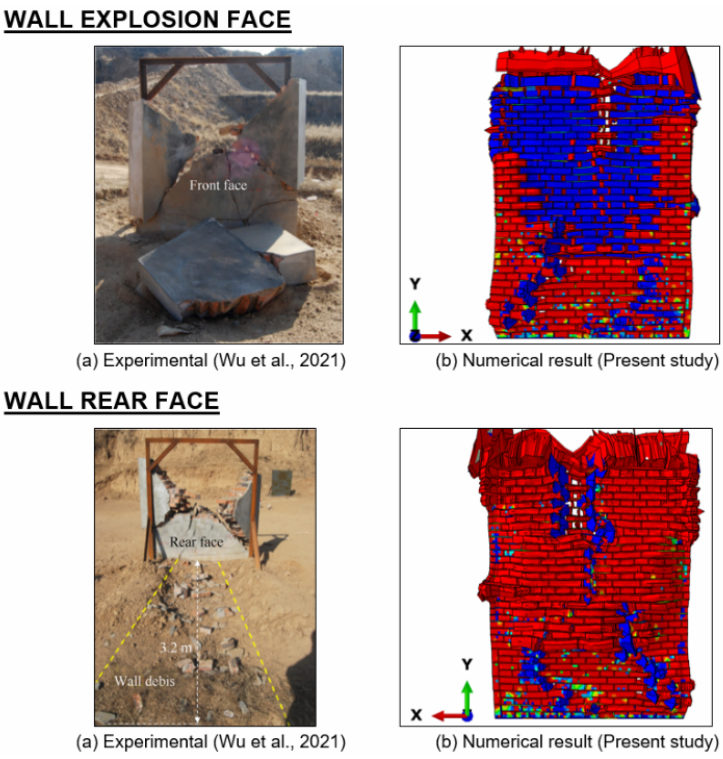

Figure 4 Different FE models' transverse Z-displacement (mm), (a) US (b) S-2.5-SWM-R (c) S-3.5-SWM-R (d) S-4.5-SWM-R (e) S-2.5-SWM-B (f) S-3.5-SWM-B (g) S-4.5-SWM-B (h) S-0.5-CFRP-R (i) S-0.6-CFRP-R (j) S-0.3-CFRP-B (see online version for colours)

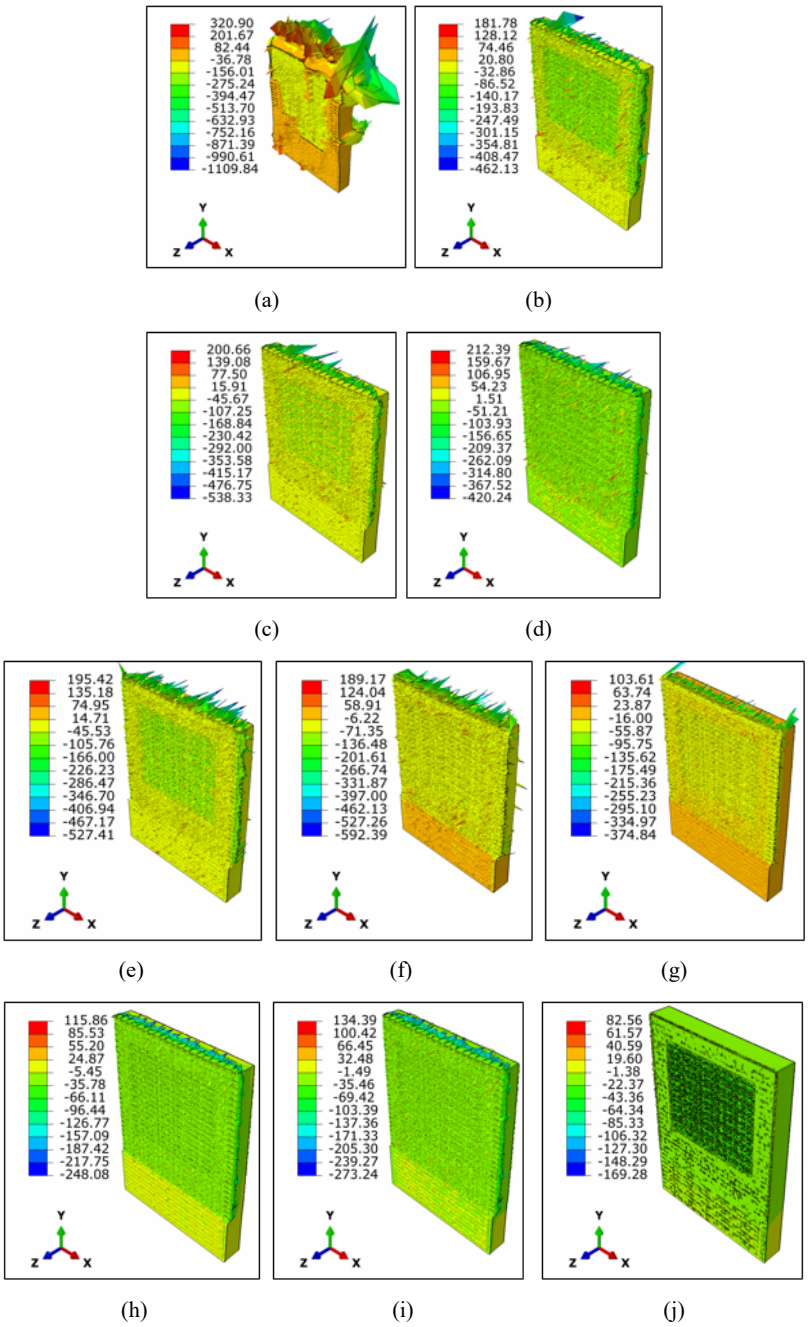

Figure 5 Damage in different walls, (a) US (b) S-2.5-SWM-R (c) S-3.5-SWM-R (d) S-4.5-SWM-R (e) S-2.5-SWM-B (f) S-3.5-SWM-B (g) S-4.5-SWM-B (h) S-0.5-CFRP-R (i) S-0.6-CFRP-R (j) S-0.3-CFRP-B (see online version for colours)

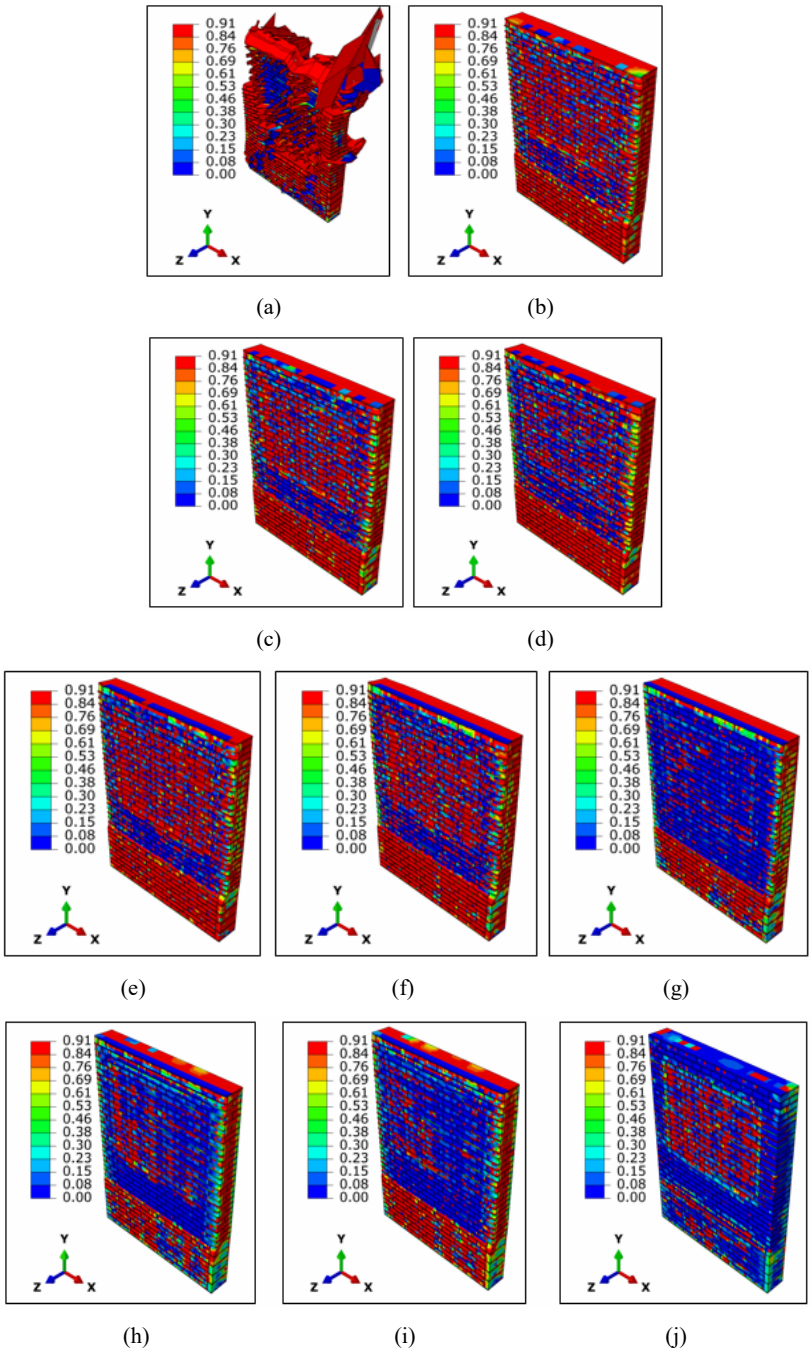

Figure 6 Principle stress distribution in bricks of several wall models under consideration, (a) US (b) S-2.5-SWM-R (c) S-3.5-SWM-R (d) S-4.5-SWM-R (e) S-2.5-SWM-B (f) S-3.5-SWM-B (g) S-4.5-SWM-B (h) S-0.5-CFRP-R (i) S-0.6-CFRP-R (j) S-0.3-CFRP-B (see online version for colours)

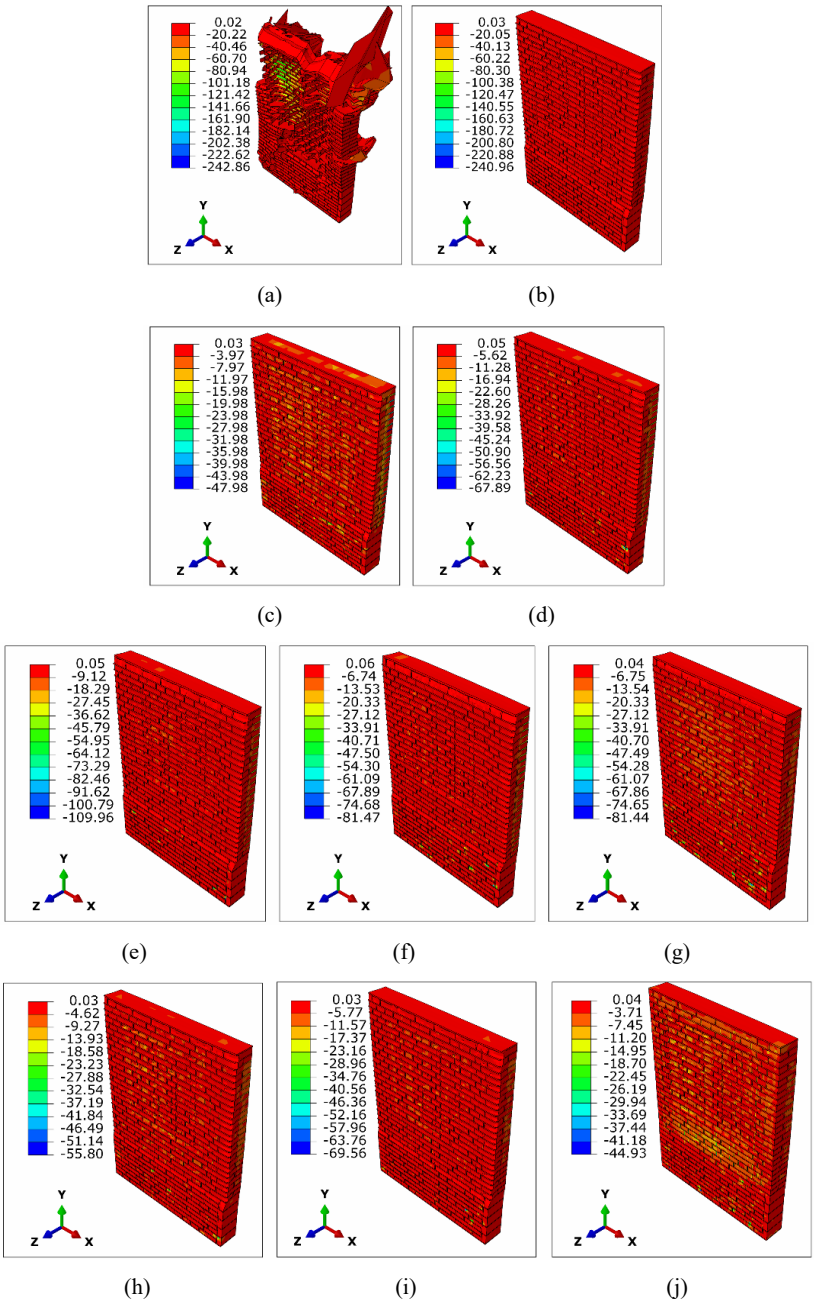

Figure 7 Stress profiles of sheet and wrapping (see online version for colours)

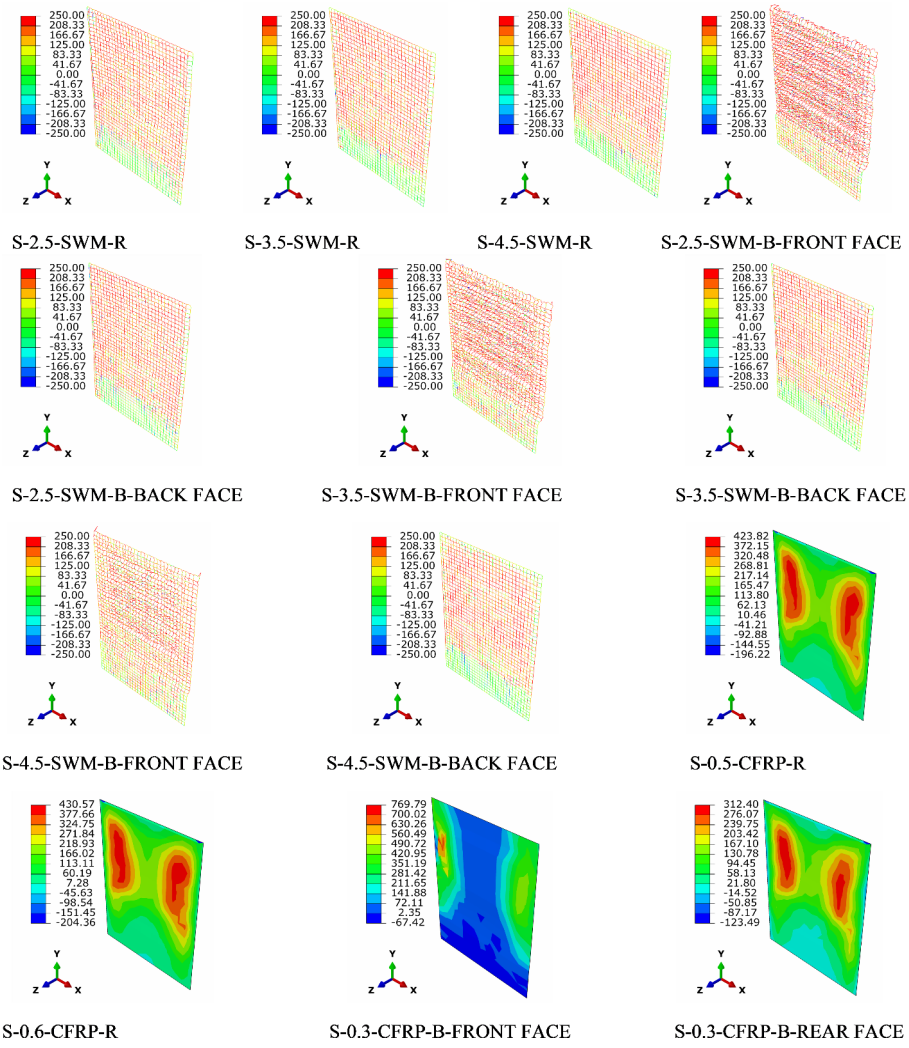

5.2 Response of wall strengthened with steel wire mesh on both faces

- Walls S-2.5-SWM-B, S-3.5-SWM-B, and S-4.5-SWM-B have steel wire mesh applied to both faces that reduces the maximum transverse displacement of the walls by 14.35%, 19.16%, and 38.87%, respectively, in comparison to walls S-2.5-SWM-R, S-3.5-SWM-R, and S-4.5-SWM-R, Figure 4.
- Compared to the walls S-2.5-SWM-R, S-3.5-SWM-R, and S-4.5-SWM-R, the compressive and shear stresses of the S-2.5-SWM-B, S-3.5-SWM-B, and

S-4.5-SWM-B walls are reduced by 8.77%, 15.33%, and 20.07%, respectively, and by 33.05%, 17.91%, and –2.6%, respectively.

- According to Figure 7, the tensile stress on the top side of the back face of the wall with mesh on both faces is 208.33 MPa in 2.5 mm diameter. It decreases as the diameter rises, reaching 166.67 MPa in 3.5 mm and 125 MPa in 4.5 mm. The tensile stresses are shown to be lowering when the mesh is applied to both faces of the wall, as opposed to applying it to the wall's back face only.
- The brittle reaction of the reinforced wall is what is responsible for the increase in shear stress of the wall with 4.50 mm wire mesh on both faces.

5.3 C-FRP strengthened masonry walls

- When C-FRP is applied to the walls S-0.5-C-FRP-R, S-0.6-C-FRP-R, and S-0.3-C-FRP-B, Figure 4 shows that the maximum transverse displacement is reduced by 64.96%, 74.77%, and 76.62%, respectively, in comparison to the un-strengthened wall.
- Figure 4 shows that the wall with the 4.50 mm thick wire mesh sustains substantially less damage than the wall with the C-FRP, despite the maximum transverse displacement of the wall S-0.5-C-FRP-R being extremely similar to the displacement of the wall S-4.5-SWM-B (95.75 mm).
- The formation of extremely high in-plane stresses in the material of the sheet is what causes the enormous DDE of the reinforced wall made of C-FRP.

6 Conclusions

In the study, the following findings are drawn:

- Due to improper and inefficient brick layering during building of the wall and significant displacement, an unreinforced masonry wall sustains severe asymmetrical damage. The use of wire mesh on the back face not only prevents damage but also evenly distributes the intense masonry stresses throughout practically the whole wall. This causes the wall's displacement to decrease. Greater wire mesh diameter further reduces the masonry's stresses, resulting in less wall movement.
- The displacement is reduced when wire mesh is applied to the front face of a wall that already has mesh on the back face. In comparison to the 4.50 mm diameter mesh, the 2.50 mm and 3.50 mm diameter wire meshes on the front face of the wall are badly torn. The wire mesh on the front face can be thought of as sacrificial mesh since it dissipates energy.
- The C-FRP sheet on the wall's two faces is discovered to be a more efficient strengthening material to enhance the masonry wall's blast performance. The sheet may have served as a sacrificial layer to shield the wall from major damage and might have been changed out for a fresh one before it was exposed to more impulsive stresses.

- It is discovered that the wall responds comparably to the blast loading taken into account in this study when 4.50 mm wire mesh is applied to both faces and 0.50 mm C-FRP sheet is applied to the back face.

References

Aamir, M., Alam, M. and Anas, S.M. (2022) 'Effect of blast location and explosive mass on the dynamic behavior of a bowstring steel highway girder bridge subjected to air-blast', *Materials Today: Proceedings*, Elsevier, https://doi.org/10.1016/j.matpr.2022.08.275 (article in press).

ABAQUS/CAE FEA Program (2017) *Concrete-Damaged Plasticity Model, Explicit Solver, Three-Dimensional Solid Element Library*, ABAQUS DS-SIMULIA User Manual.

Ahmadi, E., Alam, M. and Anas, S.M. (2021) 'Blast performance of RCC slab and influence of its design parameters', in Kolathayar, S., Ghosh, C., Adhikari, B.R., Pal, I. and Mondal, A. (Eds.): *Resilient Infrastructure, Lecture Notes in Civil Engineering*, Vol. 202, pp.389–402, Springer, Singapore, https://doi.org/10.1007/978-981-16-6978-1_31.

Ahmadi, E., Alam, M. and Anas, S.M. (2022) 'Behavior of C-FRP laminate strengthened masonry and unreinforced masonry compound walls under blast loading, Afghanistan scenario', *International Journal of Masonry Research and Innovation*, DOI: 10.1504/IJMRI. 2022.10049968 (article in press).

Anas, S.M. and Alam, M. (2021a) 'Air-blast response of free-standing: (1) unreinforced brick masonry wall, (2) cavity RC wall, (3) RC walls with (i) bricks, (ii) sand, in the cavity: a macro-modeling approach', in Marano, G.C., Ray Chaudhuri, S., Unni Kartha, G., Kavitha, P.E., Prasad, R. and Achison R.J. (Eds.): *Proceedings of SECON'21. SECON 2021. Lecture Notes in Civil Engineerin*g, Vol. 171, pp.921–930, Springer, Cham, https://doi.org/10.1007/978-3-030-80312-4_78.

Anas, S.M. and Alam, M. (2021b) 'Comparison of existing empirical equations for blast peak positive overpressure from spherical free air and hemispherical surface bursts', *Iranian Journal of Science Technology, Transactions of Civil Engineering*, Vol. 46, pp.965–984, https://doi.org/10.1007/s40996-021-00718-4.

Anas, S.M. and Alam, M. (2022a) 'Close-range blast response prediction of hollow circular concrete columns with varied hollowness ratio, arrangement of compression steel, and confining stirrups' spacing', *Iranian Journal of Science and Technology, Transactions of Civil Engineering*, https://doi.org/10.1007/s40996-022-00951-5 (article in press).

Anas, S.M. and Alam, M. (2022b) 'Dynamic behavior of free-standing unreinforced masonry and composite walls under close-range blast loadings: a finite element investigation', *International Journal of Masonry Research and Innovation*, (article in press).

Anas, S.M. and Alam, M. (2022c) 'Performance of brick-filled reinforced concrete composite wall strengthened with C-FRP laminate(s) under blast loading', *Materials Today: Proceedings*, Elsevier, https://doi.org/10.1016/j.matpr.2022.03.162.

Anas, S.M. and Alam, M. (2022d) 'Performance of simply supported concrete beams reinforced with high-strength polymer re-bars under blast-induced impulsive loading', *International Journal of Structural Engineering*, Vol. 12, No. 1, pp.62–76, http://doi/abs/10.1504/ IJSTRUCTE.2022.119289.

Anas, S.M. and Alam, M. (2022e) 'Role of shear reinforcements on the punching shear resistance of two-way RC slab subjected to impact loading', *Materials Today: Proceedings*, Elsevier, https://doi.org/10.1016/j.matpr.2022.08.510 (article in press).

Anas, S.M, Alam, M. and Umair, M. (2020a) 'Performance of one-way composite reinforced concrete slabs under explosive-induced blast loading', *IOP Conference Series: Earth and Environmental Science, Volume 614, 1st International Conference on Energetics, Civil and Agricultural Engineering*, Tashkent, Uzbekistan, https://doi.org/10.1088/1755-1315/614/1/012094.

Anas, S.M., Alam, M. and Umair, M. (2020b) 'Performance of one-way concrete slabs reinforced with conventional and polymer re-bars under air-blast loading', in Chandrasekaran, S., Kumar, S. and Madhuri, S. (Eds.): *Recent Advances in Structural Engineering. Lecture Notes in Civil Engineering*, Vol. 135, pp.179–191, https://doi.org/10.1007/978-981-33-6389-2_18.

Anas, S.M., Ansari Md, I. and Alam, M. (2020c) 'Performance of masonry heritage building under air-blast pressure without and with ground shock', *Australian Journal of Structural Engineering*, Vol. 21, No. 4, pp.329–344, https://doi.org/10.1080/13287982.2020.1842581.

Anas, S.M., Alam, M. and Umair, M. (2021a) 'Air-blast and ground shockwave parameters, shallow underground blasting, on the ground and buried shallow underground blast-resistant shelters: a review', *International Journal of Protective Structures*, Vol. 13, No. 1, pp.99–139, https://doi.org/10.1177/2F20414196211048910.

Anas, S.M., Alam, M. and Umair, M. (2021b) 'Influence of charge locations on close-in air-blast response of pre-tensioned concrete U-girder', in Kolathayar, S., Ghosh, C., Adhikari, B.R., Pal, I. and Mondal, A. (Eds.): *Resilient Infrastructure, Lecture Notes in Civil Engineering*, Vol. 202, pp.513–527, Springer, Singapore, https://doi.org/10.1007/978-981-16-6978-1_40.

Anas, S.M., Alam, M. and Umair, M. (2021c) 'Experimental and numerical investigations on performance of reinforced concrete slabs under explosive-induced air-blast loading: a state-of-the-art review', *Structures*, Vol. 31, pp.428–461, Elsevier, https://doi.org/10.1016/j.istruc.2021.01.102.

Anas, S.M., Alam, M. and Umair, M. (2021d) 'Out-of-plane response of clay brick unreinforced and strengthened masonry walls under explosive-induced air-blast loading', in Kolathayar, S., Ghosh, C., Adhikari, B.R., Pal, I. and Mondal, A. (Eds.): *Resilient Infrastructure, Lecture Notes in Civil Engineering*, Vol. 202, pp.477–491, Springer, Singapore, https://doi.org/10.1007/978-981-16-6978-1_37.

Anas, S.M., Alam, M. and Umair, M. (2021e) 'Performance of on-ground double-roof RCC shelter with energy absorption layers under close-in air-blast loading', *Asian Journal of Civil Engineering*, Vol. 22, pp.1525–1549, https://doi.org/10.1007/s42107-021-00395-8.

Anas, S.M., Ansari Md, I. and Alam, M. (2021f) 'A study on existing masonry heritage building to explosive-induced blast loading and its response', *International Journal of Structural Engineering*, Vol. 11, No. 4, pp.387–412, http://doi/abs/10.1504/IJSTRUCTE.2021.118065.

Anas, S.M., Alam, M. and Alam, M. (2022a) 'Performance prediction of axially loaded square reinforced concrete column with additional transverse reinforcements in the form of (1) master ties, (2) diamond ties, and (3) open ties under close-in blast', in Pal, I. et al. (Eds.): *Proceedings of the 2nd International Symposium on Disaster Resilience and Sustainable Development, Lecture Notes in Civil Engineering*, Springer, Vol. 294, https://doi.org/10.1007/978-981-19-6297-4_12 (article in press).

Anas, S.M., Alam, M. and Alam, M. (2022b) 'Reinforced cement concrete (RCC) shelter and prediction of its blast loads capacity', *Materials Today: Proceedings*, Elsevier, (article in press).

Anas, S.M., Alam, M. and Shariq, M. (2022c) 'Behavior of two-way RC slab with different reinforcement orientation layouts of tension steel under drop load impact', *Materials Today: Proceedings*, Elsevier, https://doi.org/10.1016/j.matpr.2022.08.509 (article in press).

Anas, S.M., Alam, M. and Shariq, M. (2022d) 'Damage response of conventionally reinforced two-way spanning concrete slab under eccentric impacting drop weight loading', *Defence Technology*, https://doi.org/10.1016/j.dt.2022.04.011.

Anas, S.M., Alam, M. and Tahzeeb, R. (2022e) 'Impact response prediction of square RC slab of normal strength concrete strengthened with (1) laminates of (i) mild-steel and (ii) C-FRP, and (2) strips of C-FRP under falling-weight load', *Materials Today: Proceedings*, Elsevier, https://doi.org/10.1016/j.matpr.2022.07.324, (article in press).

Anas, S.M., Alam, M. and Umair, M. (2022f) 'Air-blast response of axially loaded clay brick masonry walls with and without reinforced concrete core', in Fonseca de Oliveira Correia, J.A. et al. (Eds.): *ASMA 2021, Advances in Structural Mechanics and Applications, STIN 19*, pp.1–18, 2023, https://doi.org/10.1007/978-3-030-98335-2_4 (article in press).

Anas, S.M., Alam, M. and Umair, M. (2022g) 'Effect of design strength parameters of conventional two-way singly reinforced concrete slab under concentric impact loading' *Materials Today: Proceedings*, Elsevier, https://doi.org/10.1016/j.matpr.2022.02.441.

Anas, S.M., Alam, M. and Umair, M. (2022h) 'Experimental studies on blast performance of unreinforced masonry (URM) walls of clay bricks and concrete blocks: a state-of-the-art review', *International Journal of Masonry Research and Innovation*, DOI: 10.1504/IJMRI.2022.10049719 (article in press)

Anas, S.M., Alam, M. and Umair, M. (2022i) 'Performance based strengthening with concrete protective coatings on braced unreinforced masonry wall subjected to close-in explosion', *Materials Today: Proceedings*, Elsevier, https://doi.org/10.1016/j.matpr.2022.04.206.

Anas, S.M., Alam, M. and Umair, M. (2022j) 'Performance of (1) concrete-filled double-skin steel tube with and without core concrete, and (2) concrete-filled steel tubular axially loaded composite columns under close-in blast', *International Journal of Protective Structures*, https://doi.org/10.1177/2F20414196221104143.

Anas, S.M., Alam, M. and Umair, M. (2022k) 'Performance prediction of braced unreinforced and strengthened clay brick masonry walls under close-range explosion through numerical modeling', *International Journal of Computational Materials Science and Surface Engineering*, (article in press).

Anas, S.M., Alam, M. and Umair, M. (2022l) 'Role of UHPC in-lieu of ordinary cement-sand plaster on the performance enhancement of masonry wall under close-range blast loading: a finite element investigation', *International Journal of Masonry Research and Innovation*, (article in press).

Anas, S.M., Alam, M. and Umair, M. (2022m) 'Strengthening of braced unreinforced brick masonry wall with (i) C-FRP wrapping, and (ii) steel angle-strip system under blast loading', *Materials Today: Proceedings*, Elsevier, https://doi.org/10.1016/j.matpr.2022.01.335.

Anas, S.M., Alam, M., Umair, M. and Kanaan, M.H.G. (2022n) 'Strengthening of unreinforced braced masonry wall with (1) CFRP laminate and (2) mild-steel strips: innovative techniques, against close-range explosion', *International Journal of Masonry Research and Innovation*, (article in press).

Anas, S.M., Shariq, M. and Alam, M. (2022o) 'Performance of axially loaded square RC columns with single/double confinement layer(s) and strengthened with C-FRP wrapping under close-in blast', *Materials Today: Proceedings*, Elsevier, https://doi.org/10.1016/ j.matpr.2022.01.275.

Anas, S.M., Shariq, M., Alam, M. and Umair, M. (2022p) 'Evaluation of critical damage location of contact blast on conventionally reinforced one-way square concrete slab applying CEL-FEM blast modeling technique', *International Journal of Protective Structures*, https://doi.org/10.1177/2F20414196221095251.

ASCE/SEI 59-11(2011) *Blast Protection of Buildings*, American Society of Civil Engineers, USA.

Badshah, E., Naseer, A., Ashraf, M. and Ahmad, T. (2021) 'Response of masonry systems against blast loading', *Defence Technology*, Vol. 17, No. 2021, pp.1326–1337.

Ehsani, M. and Pena, C.S. (2009) 'Blast loading retrofit of unreinforced masonry walls', *Structural Magazine*, pp.16–20.

Goel, D.M. and Matsagar, A.V. (2014) 'Blast-resistant design of structures', *Practice Periodical on Structural Design and Construction*, Vol. 19, No. 2, pp.1–9, ASCE.

Hadi Ghaffoori Kanaan, M., Jebur Obayes Al-Isawi, A. and Ahmad Mohamme, F. (2022) 'Antimicrobial resistance and antibiogram of thermotolerant campylobacter recovered from poultry meat in Baghdad Markets, Iraq', *Archives of Razi Institute*, Vol. 77, No. 1, pp.231–237, DOI: 10.22092/ARI.2021.356362.1828.

Hafezolghorani, M., Hejazi, F., Vaghei, R., Saleh, M. and Karimzade, K. (2017) 'Simplified damage plasticity model for concrete', *Structural Engineering International*, Vol. 27, No. 1, pp.68–78.

Hao, H. and Tarasov, B. (2008) 'Experimental study of dynamic material properties of clay brick and mortar at different strain rates', *Aust. J. Struct. Eng.*, Vol. 8, No. 1, pp.117–131.

Hao, H., Hao, Y., Li. J. and Chen, W. (2016) 'Review of the current practices in blast resistant analysis and design of concrete structures', *Advances in Structural Eng.*, Vol. 19, No. 8, pp.1193–1223.

IS 4948 (2002) *Welded Steel Wire Fabric for General Use*, Bureau of Indian Standards, New Delhi, India.

Kanaan, M. and Abdullah, S. (2021) 'Evaluation of aqueous ozone as a method to combat multidrug-resistant staphylococcus aureus tainting cattle meat sold in Wasit marketplaces', *Mansoura Veterinary Medical Journal*, Vol. 22, No. 3, pp.117–123, DOI: 10.21608 /MVMJ.2021.196988.

Kanaan, M.H. (2018) 'Antibacterial effect of ozonated water against methicillin-resistant Staphylococcus aureus contaminating chicken meat in Wasit Province, Iraq', *Veterinary World*, Vol. 11, No. 10, pp.1440–1445, DOI: 10.14202/vetworld.2018.1445-1453.

Kanaan, M.H. (2021) 'Prevalence, resistance to antimicrobials, and antibiotypes of Arcobacter species recovered from retail meat in Wasit marketplaces in Iraq', *Int. J. One Health*, Vol. 7, pp.142–150, DOI: 10.14202/IJOH.2021.142-150.

Kanaan, M.H.G. and Abdulwahid, M.T. (2019) 'Prevalence rate, antibiotic resistance and biotyping of thermotolerant campylobacter isolated from poultry products vended in Wasit markets', *Current Research in Nutrition and Food Science Journal*, Vol. 7, No. 3, pp.905–917, DOI: 10.12944/CRNFSJ.7.3.29.

Kanaan, M.H.G. and Al-Isawi, A.J.O. (2019) 'Prevalence of methicillin or multiple drug-resistant staphylococcus aureus in cattle meat marketed in Wasit province', *Biochem. Cell. Arch.*, Vol. 19, No. 1, pp.495–502, DOI: 10.35124/bca.2019.19.1.495.

Kanaan, M.H.G. and Khashan, H.T. (2022) 'Molecular typing, virulence traits and risk factors of pandrug-resistant Acinetobacter baumannii spread in intensive care unit centers of Baghdad city, Iraq', *Reviews in Medical Microbiology*, Vol. 33, No. 1, pp.51–55, DOI: 10.1097/MRM.0000000000000282.

Kanaan, M.H.G. and Tarek, A.M. (2020) 'Clostridium botulinum, a foodborne pathogen and its impact on public health', *Annals of Tropical Medicine and Public Health*, Vol. 23, pp.49–62, DOI: 10.36295/ASRO.2020.2357.

Kanaan, M.H., Anah, G., Jasim, G.A. and Ghasemian, A. (2020a) 'In-vitro protoscolicidal and immunomodulatory effects of Cinnamomum camphora and Ziziphora tenuior against Echinococcus granulosus protoscolices', *Reviews in Medical Microbiology*, July 20, DOI: 10.1097/MRM.0000000000000221.

Kanaan, M.H.G., Al-Shadeedi, S.M., Al-Massody, A.J. and Ghasemian, A. (2020b) 'Drug resistance and virulence traits of Acinetobacter baumannii from Turkey and chicken raw meat', *Comparative Immunology, Microbiology and Infectious Diseases*, Vol. 70, p.101451, DOI: 10.1016/j.cimid.2020.101451.

Kanaan, M.H.G., Tarek, A.M. and Abdullah, S.S. (2021) 'Knowledge and attitude among samples from community members, pharmacists and health care providers about antibiotic resistance in Al-Suwaria city/Wassit province/Iraq', in *IOP Conference Series: Earth and Environmental Science*, IOP Publishing, June, Vol. 790, No. 1, p.012059, DOI: 10.1088/1755-1315/790/1/012059.

Milani, G. and Lourenco, P.B. (2009) 'Blast analysis of enclosure masonry walls using homogenization approaches', *Multiscale Computational Engineering*, Vol. 7, No. 2, pp.91–113.

Milani, G., Lourenco, P.B. and Tralli, A. (2009) 'Homogenized rigid.plastic model for masonry walls subjected to impact', *International Journal of Solids and Structures*, Vol. 46, Nos. 22–23, pp.4133–4149.

Myers, J.J., Belarbi, A. and Domiaty, K.A. (2004) 'Blast resistance of FRP retrofitted un-reinforced masonry (URM) walls with and without arching action', *TMS Journal*, August, Vol. 6, No. 1, pp.9–26.

Pandey, A.K. and Bisht, R.S. (2014) 'Numerical modelling of infilled clay bricks masonry under blast loading', *Advances in Structural Engineering*, Vol. 17, No. 4, pp.591–606.

Phan-Vu, P.T., Tran, D.M., Pham, T.D., Dang, T., Ngo-Huu, C. and Nguyen-Minh, L. (2021) 'Distinguished bond behaviour of C-FRP sheets in unbonded post-tensioned rein-forced concrete beams versus single-lap shear tests', *Engineering Structures*, Vol. 234, No. 1, pp.1–13, Elsevier.

Shamim, S., Ahmad, S. and Khan, A.K. (2019) 'Finite element analysis of masonry wall subjected to blast loading', *International Journal of Advances in Mechanical and Civil Engineering*, Vol. 16, No. 1, pp.40–43.

Shariq, M., Alam, M. and Husain, A. (2022a) 'Performance of RCC column retrofitted with C-FRP wrappings and the wrappings with steel angle-batten jacketing under blast loading', in Nandagiri, L., Narasimhan, M.C. and Marathe, S. (Eds.): *Recent Advances in Civil Engineering, Lecture Notes in Civil Engineering*, Vol. 256, Springer, Singapore, https://doi.org/10.1007/978-981-19-1862-9_21.

Shariq, M., Alam, M., Anas, S.M., Islam, N. and Hussain, A. (2022b) 'Performance enhancement of square RC column carrying axial compression by (1) C-FRP wrapping, and (2) steel angle system under air-blast loading', *International Journal of Computational Materials Science and Surface Engineering*, (article in press).

Shariq, M., Alam, M., Husain, A. and Anas, S.M. (2022c) 'Jacketing with steel angle sections and wide battens of RC column and its influence on blast performance', *Asian Journal of Civil Engineering*, Springer, https://doi.org/10.1007/s42107-022-00437-9.

Shariq, M., Alam, M., Husain, A. and Islam, N. (2022d) 'Response of strengthened unreinforced brick masonry wall with (1) mild steel wire mesh and (2) C-FRP wrapping, under close-in blast', *Materials Today: Proceedings*, Elsevier, https://doi.org/10.1016/j.matpr.2022.05.153.

Shariq, M., Anas, S.M. and Alam, M. (2022e) 'Blast resistance prediction of clay brick masonry wall strengthened with steel wire mesh, and C-FRP laminate under explosion loading: a finite element analysis', *International Journal of Reliability and Safety*, (article in press).

Shariq, M., Saifi, F., Alam, M. and Anas, S.M. (2022f) 'Effect of concrete strength on the dynamic behavior of axially loaded reinforced concrete column subjected to close-range explosive loading', *Materials Today: Proceedings*, Elsevier, https://doi.org/10.1016/j.matpr.2022.07.313, (article in press).

Stewart, M.G. and Lawrence, S. (2002) 'Struct reliability of masonry walls in flexure', *Int. J. Masonry*, Vol. 15, No. 2, pp.48–52.

Tahzeeb, R., Alam, M. and Mudassir, S.M. (2022a) 'A comparative performance of columns: reinforced concrete, composite, and composite with partial C-FRP wrapping under contact blast', *Materials Today: Proceedings*, Elsevier, https://doi.org/10.1016/j.matpr.2022.03.367.

Tahzeeb, R., Alam, M. and Mudassir, S.M. (2022b) 'Effect of transverse circular and helical reinforcements on the performance of circular RC column under high explosive loading', *Materials Today: Proceedings*, Elsevier, https://doi.org/10.1016/j.matpr.2022.04.676.

Tahzeeb, R., Alam, M. and Mudassir, S.M. (2022c) 'Performance of composite and tubular columns under close-in blast loading: a comparative numerical study', *Materials Today: Proceedings*, Elsevier, https://doi.org/10.1016/j.matpr.2022.04.587.

TM 5-1300(1990) *Structures to Resist the Effect of Accidental Explosions*, Technical manual, Joint Department of the Army, the Navy, and the Air Force, USA.

Ul Ain, Q., Alam, M. and Anas, S.M. (2021) 'Behavior of ordinary load-bearing masonry structure under distant large explosion, beirut scenario', in Kolathayar, S., Ghosh, C., Adhikari, B.R., Pal, I. and Mondal, A. (Eds.): *Resilient Infrastructure, Lecture Notes in Civil Engineering*, Vol. 202, pp.239-253, Springer, Singapore, https://doi.org/10.1007/978-981-16-6978-1_19.

Ul Ain, Q., Alam, M. and Anas, S.M. (2022) 'Response of two-way RCC slab with unconventionally placed reinforcements under contact blast loading', in Fonseca de Oliveira Correia, J.A. et al. (Eds.): *ASMA 2021, Advances in Structural Mechanics and Applications, STIN 19*, 2023, pp.1–18, https://doi.org/10.1007/978-3-031-04793-0_17 (article in press).

Voyiadjis, G.Z., Taqieddin, Z.N. and Kattan, P.I. (2008) 'Anisotropic damage-plasticity model for concrete', *International Journal of Plasticity*, Vol. 24, No. 1, pp.1946–1965.

Wei, J., Du, Z., Zheng, Y. and Ounhueane, O. (2021) 'Research on damage characteristics of bricks masonry under explosion load', *Shock and Vibration*, Article ID: 5519231, Vol. 2021, No. 1, pp.15–30.

Wei, X. and Stewart, M.G. (2010) 'Model validation and parametric study on the blast response of unreinforced brick masonry walls', *International Journal of Impact Engineering*, Vol. 37, No. 1, pp.1150–1159.

Wu, C. and Hao, H. (2005) 'Modelling of simultaneous ground shock and air blast pressure on nearby structures from surface explosions', *International Journal of Impact Engineering*, Vol. 31, No. 1, pp.699–717.

Wu, G., Ji, C., Wang, X., Gao, F., Zhao, C., Liu, Y. and Yang, G. (2021) 'Blast response of clay brick masonry unit walls unreinforced and reinforced with polyurea elastomer', *Defence Technology*, Article in press.